Properties of crystallizing soft sphere systems

1999 J. Phys.: Condens. Matter 11 10133

(http://iopscience.iop.org/0953-8984/11/50/307)

J. Phys.: Condens. Matter **11** (1999) 10133–10141. Printed in the UK PII: S0953-8984(99)06931-3

Properties of crystallizing soft sphere systems

Dean C Wang and Alice P Gast†

Department of Chemical Engineering, Stanford University, Stanford, CA 94305-5025, USA

E-mail: alice@chemeng.stanford.edu

Received 13 August 1999, in final form 8 October 1999

Abstract. In this paper, we explore the similar behaviour of the Yukawa and power law systems at crystallization. This is done within the context of our density functional theory model, the modified weighted density approximation with a static solid reference state. Some issues we probe include the stable solid crystalline structure at equilibrium, the fractional change in density upon crystallization, the Lindemann ratio of the equilibrium solid and the magnitude of the first peak of the structure factor at freezing. We find many similarities between these two classes of potentials. We also compare our findings with computer simulation and experimental results. While the theoretical and simulation results in general agree, there exists some discrepancies between these results for the Yukawa system and the experimental findings for colloidal suspensions.

1. Introduction

Many complex fluid systems undergo an ordering transition as density is increased [1]. Examples include opals, star polymers, soap micelles and proteins. Often these systems comprise micelles, macroion particles or polymers, and their interaction energies can be characterized as soft sphere repulsions. Two important soft sphere interaction potentials are the Yukawa and power law (or inverse nth power) models. The Yukawa potential for charged particles of valence Z is given by:

$$U = \Gamma \frac{\mathrm{e}^{-\lambda r/a}}{r/a} \tag{1}$$

where Γ is the coupling parameter $= (Ze)^2/\varepsilon a$ where Z is the valence, e is the electron charge, ε is the dielectric constant of the medium and $a = \rho^{-1/3}$ is the average interparticle distance at a density ρ. The $1/r$ electrostatic repulsion is screened, and thus has an exponential cutoff determined by $\lambda = \kappa a$ where κ^{-1} is the Debye screening length determined by the ionic strength of the medium [2].

The power law potential:

$$U = 4\varepsilon \left(\frac{\sigma}{r}\right)^n \tag{2}$$

where n can vary from ∞ for the short-range hard sphere system to one for the long-range one-component plasma (OCP) has been used to describe metallic liquids [3–5], Lennard-Jones systems at high temperatures [6] and sometimes serves as the repulsive reference state of perturbation theories [7, 8].

† Corresponding author.

0953-8984/99/5010133+09$30.00

Despite their different mathematical forms, the Yukawa and power law systems both exhibit many similar qualitative behaviours at crystallization. Both fluids freeze into face-centred cubic (FCC) solids for short-range, harder (large κ or n) potentials, but body-centred cubic (BCC) solids for longer-range, softer (small κ or n) potentials. The fractional change upon freezing is comparable for both systems and decreases as the repulsion softens. The Lindemann parameter, a measure of the vibrations present in a solid, is roughly constant across the different ranges and hardnesses within each system at the melting point.

In this short paper, we will explore some of the similarities between the two systems, focusing on the structural properties at crystallization, such as the equilibrium solid structure, the magnitude of the density change and the values of the Lindemann parameter. We will discuss these aspects within the context of our density functional theory model which will be briefly summarized in the next section.

2. Density functional theory of crystallization

The density functional theory formalism we employ is our modified weighted density approximation (MWDA) with a static solid reference state. This model has been described before [9–11] and therefore only a very brief summary will be given here. The reader is urged to consult previous papers on its background and its relationship with the basic modified weighted density approximation [9, 12, 13].

In density functional theory, the total Helmholtz free energy is taken to be a functional of the local density $\rho(\boldsymbol{r})$ and is generally decomposed into ideal and excess components:

$$F[\rho] = F_{ideal}[\rho] + F_{excess}[\rho] \tag{3}$$

with the ideal component known exactly:

$$F_{ideal}[\rho] = kT \int \mathrm{d}\boldsymbol{r}\rho(\boldsymbol{r})\{\ln[\Lambda^3\rho(\boldsymbol{r})] - 1\} \tag{4}$$

where k is the Boltzmann constant and Λ is the thermal de Broglie wavelength. The excess free energy is approximated by taking into account both the uniform liquid, as well as the perfectly ordered static solid. In this manner, it is hoped that the equilibrium solid, whose structure lies in between these two extremes, will be well modelled. This is done by writing the excess free energy

$$F_{excess}[\rho] = Nf(\bar{\rho}) \tag{5}$$

as a product of the local excess free energy of the fluid phase, $f(\bar{\rho})$, at a weighted, or coarse-grained, density and N, the number of particles. This weighted density, $\bar{\rho}$, corresponds to the *liquid* density that accurately models a *solid* with density ρ_s.

The solid is modelled with a Gaussian distribution around lattice positions $\boldsymbol{R}_i$:

$$(\bar{\rho}) = \left(\frac{\alpha}{\pi}\right)^{3/2} \sum_{\boldsymbol{R}_i} \exp(-\alpha|\boldsymbol{r} - \boldsymbol{R}_i|^2). \tag{6}$$

The localization parameter, α, varies from 0 for the uniform fluid phase to ∞ for the perfectly ordered static solid. Standard relationships from liquid state theory provide a simple algebraic relationship for the weighted density:

$$\bar{\rho}(\rho_s, \alpha) = \rho_s\left(1 - \frac{1}{2\beta f'(\bar{\rho})} \sum_{\boldsymbol{k}\neq 0} \exp(-\boldsymbol{k}^2/2\alpha)c(\boldsymbol{k}; \bar{\rho})\right) \tag{7}$$

where $\beta = 1/kT$ is the inverse temperature and $c(\boldsymbol{k}; \rho)$ is the fourier component of the liquid two-particle direct correlation function. This is evaluated by solving the Ornstein–Zernike

equation with the perturbative hypernetted chain (PHNC) equation closure of Kang and Ree [14], which is accurate for power law potentials to moderately high densities. More information about the PHNC equation can be found in [14].

Failures in the density functional theories arise from the inability to accurately model solid phase correlations with a liquid. We choose to alter the correlations in the effective liquid by moderating the indirect correlations in the Ornstein–Zernike equation used for the effective liquid through a new weighted density $\hat{\rho}$ via

$$c(r_{12};\rho) = h(r_{12};\rho) - \hat{\rho}\int c(r_{13};\rho)h(r_{23};\rho)\,\mathrm{d}\boldsymbol{r}_3 \tag{8}$$

where $\hat{\rho}$ is given in terms of the weighted densities for the perfectly ordered solid that is predicted by equation (7), $\bar{\rho}_\infty$, and its actual value, $\bar{\rho}_{static}$:

$$\frac{\hat{\rho}}{\bar{\rho}} = \frac{\rho_s - \bar{\rho}_\infty}{\rho_s - \bar{\rho}_{static}}. \tag{9}$$

Equation (7) is then solved iteratively and self-consistently for the weighted density, and the free energies can be calculated as a function of the localization parameter α. At each solid density, a minimum in the total free energy curve for a nonzero α value corresponds to a stable solid in the MWDA theory. A variation of the static solid reference state MWDA model involves taking into account the Einstein frequencies of the highly ordered solid to ensure that the free energies approach the exact Madelung values in a logical way in the high α limit [11].

3. Structural properties of soft spheres

The phase diagrams for the Yukawa and power law systems found via our density functional theory model are shown in figure 1. The variables used to describe the Yukawa system are $T^* = kT/\Gamma$ and $\lambda = \kappa a$. We note that this reduced temperature can be re-expressed in terms of the Bjerrum length $l_b = e^2/\varepsilon kT$, as $T^* = Z^{-2}(a/l_b)$, such that it represents the product of the particle charge and the interparticle spacing relative to the charge separation in the system. The power law exponent, n, and a composite variable, $X = 2^{6/n}\rho\sigma^3(\varepsilon/kT)^{3/n}/2^{1/2}$, combine temperature and density to determine the power law phase diagram. While exact quantitative comparisons between the two different systems are not possible, both λ and n can be viewed as hardness–softness parameters, while T^* and X contain the reduced temperatures and densities. As can be seen in figure 1, both systems possess a fluid phase at high temperatures or low densities (high T^* or low X), an FCC solid phase at low temperatures and large λ or n and a BCC solid phase at low temperatures and small λ or n. The triple point occurs at roughly $\lambda \sim 5.4$ and $n \sim 5.7$, corresponding to $T^* \sim 4 \times 10^{-4}$ and $X \sim 1.8$ [9, 11].

We can attempt to compare the two soft sphere phase diagrams more quantitatively by using a reduced temperature scaled on a phonon energy, $\tilde{T} = kT/ma^2\omega_E^2$, where $ma^2\omega_E^2$ is the product of the mass and the squares of the interparticle spacing and Einstein frequency. The Einstein frequency for the Yukawa system is simply related to the Debye screening length via the harmonic approximation to the potential, or $ma^2\omega_E^2 = 2\lambda^2 U_t/3$, where U_t is the total lattice energy per particle for the system [15]. The phonon energy for the power law system is also determined in the harmonic approximation from the second derivative of the pair potential, while the reduced temperature is simply related to the power exponent and the composite variable X, as $\tilde{T} = 2^{4/3}/X^{n/3}n(n+1)$. In figure 2, we illustrate these phase diagrams where we note that while they are qualitatively very similar, the crystallization boundary at the liquid–BCC–FCC triple point differs by a factor of about five.

The coexistence region in a phase diagram is very sensitive to the nature of the interaction potential and reflects the order of the phase transition. One quantitative measure of this

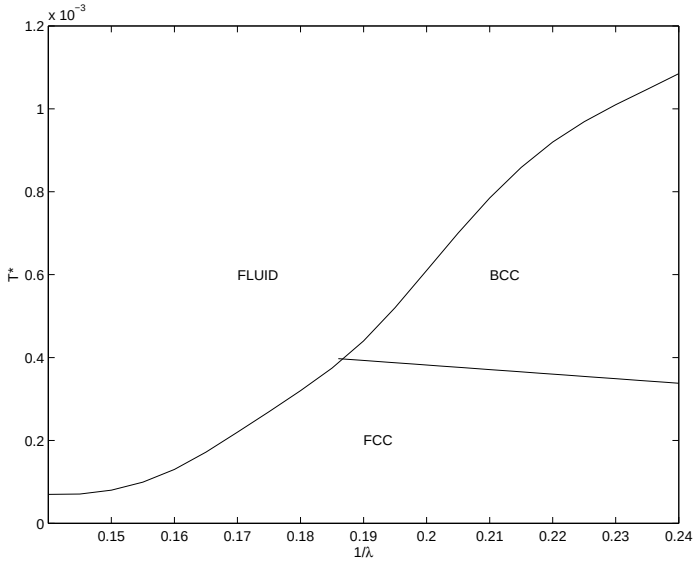

(a)

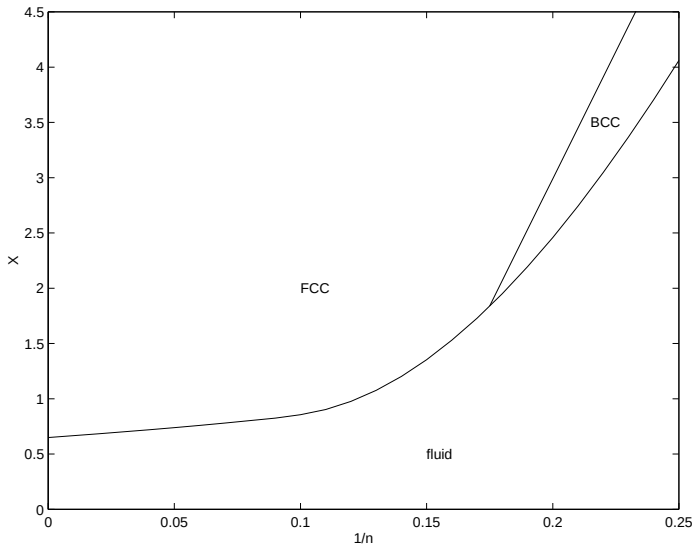

(b)

Figure 1. (a) Phase diagram of Yukawa fluid with T^* versus $1/\lambda$. (b) Phase diagram of power law fluid with X versus $1/n$.

behaviour is the fractional change in density upon freezing or $(\rho_S - \rho_F)/\rho_F$, also called the miscibility gap, where ρ_S and ρ_F are the coexisting densities of the solid and fluid phases, respectively. Interestingly, the magnitudes and trends of the fractional changes in density (or equivalently of X for the power law case) upon freezing are quantitatively comparable for both classes of potentials. This is illustrated in figure 3 where fractional change in density is plotted as a function of interaction hardness, either $1/n$ or $1/\lambda$. For the power law system, the fractional changes in density vary from less than 1% for $n = 4$ to over 4% for $n = 12$ and

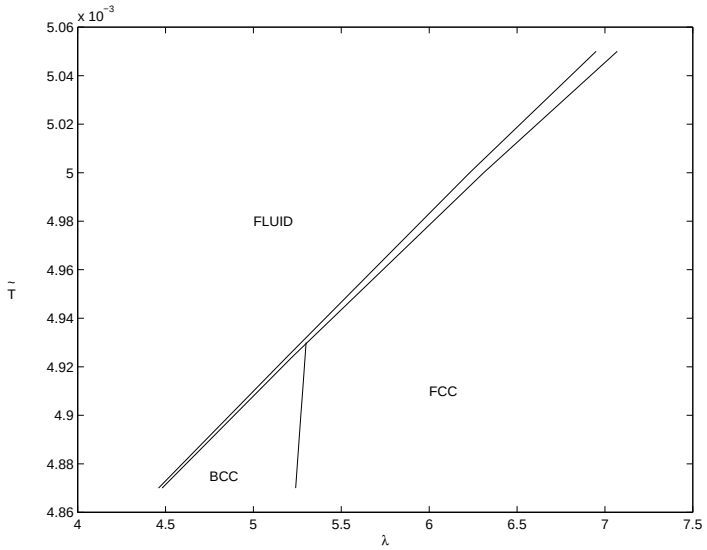

(a)

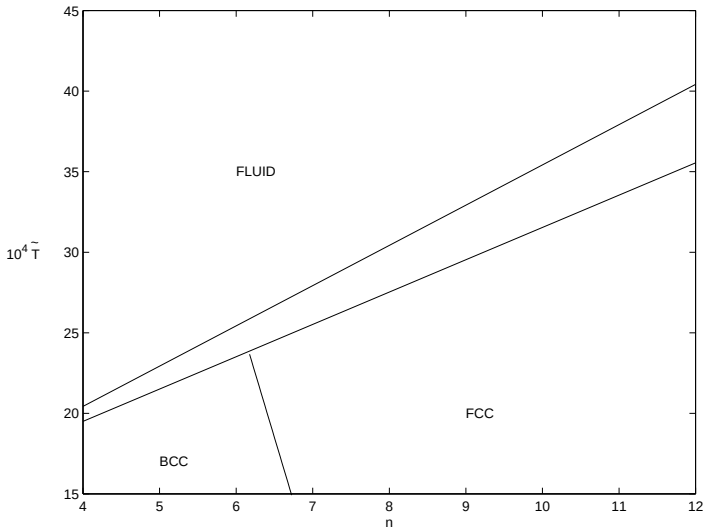

(b)

Figure 2. (a) Yukawa phase diagram with the temperature scaled on the phonon energy $\tilde{T} = 3kT/2\lambda^2 U_t$. (b) Power law phase diagram with the temperature scaled on the phonon energy $\tilde{T} = 2^{4/3}/X^{n/3}n(n+1)$.

12% in the hard sphere limit. Similarly, the Yukawa system yields values of less than 1% for $\lambda \sim 4.5$ to around 5% for $\lambda \sim 7$. These comparable values indicate that similar structural changes are probably occurring in both systems during the freezing process. In addition, the decrease in the miscibility gap as the potential becomes softer and of longer range is consistent with the prediction that this quantity should become zero in the OCP limit of isochoric freezing [16, 17]. At the liquid–BCC–FCC triple point, the miscibility gap for the two systems differs by a factor of two.

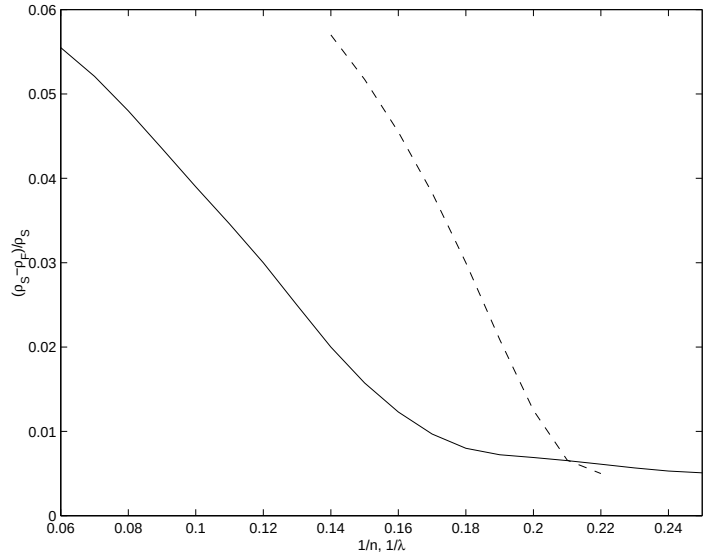

Figure 3. Fractional change in density at crystallization as a function of $1/\lambda$ for the Yukawa fluid (dashed lines) and as a function of $1/n$ for the power law fluid (solid line).

The Lindemann parameter is defined as the ratio of the mean squared displacement of a particle to the nearest neighbour distance in the solid [18]. For the FCC solid, it is given by:

$$L = \left(\frac{3}{a_{FCC}^2 \alpha}\right)^{1/2} \tag{10}$$

where $a_{FCC} = (4/\rho)^{1/3}$ is the FCC lattice constant and α is the Gaussian order parameter defined in equation (6) above. For the BCC solid, the Lindemann parameter is:

$$L = \left(\frac{2}{a_{BCC}^2 \alpha}\right)^{1/2} \tag{11}$$

where $a_{BCC} = (2/\rho)^{1/3}$ is the BCC lattice constant. For the power law potentials, we find Lindemann parameters in the range of $L = 0.13$ to $L = 0.14$ for all n [9]. For the Yukawa potentials, the value is larger, around $L = 0.22$ to $L = 0.23$ [11], but still roughly constant for all λ values studied. The empirical Lindemann rule states that a solid will melt when the Lindemann parameter reaches a value of $L = 0.10$ [18]. Although we are studying the freezing transition, the estimates for the Lindemann parameter for soft spheres are larger than that implied by the rule. This is also true, however, for the hard sphere [19] and Lennard-Jones systems [20, 21]. On the other hand, the Lindemann parameter is highly sensitive to the solid density through the lattice constant and small errors in the coexisting densities are magnified in L.

Like the Lindemann rule for melting, the empirical Hansen–Verlet rule is often used to predict the onset of crystallization. Specifically, the rule states that crystallization will occur for a system when the first peak of its structure factor reaches 2.85 in magnitude [21–23]. The structure factor is related to the Fourier component of the direct correlation function in equation (7) via

$$S(k) = \frac{1}{1 - \rho c(k)}. \tag{12}$$

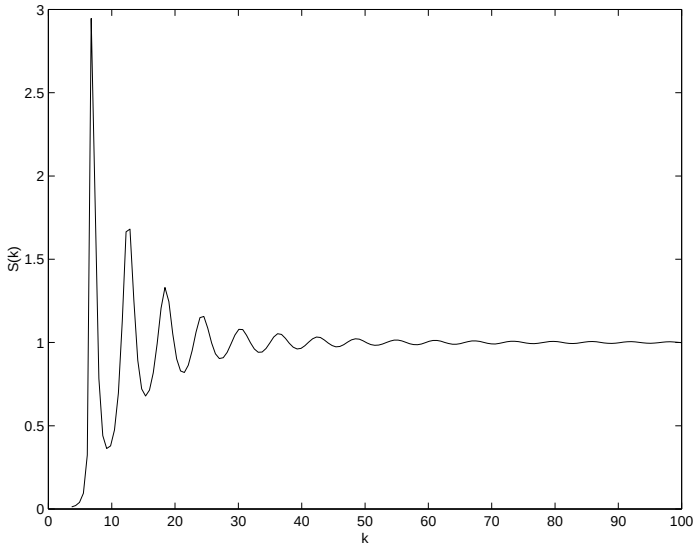

(a)

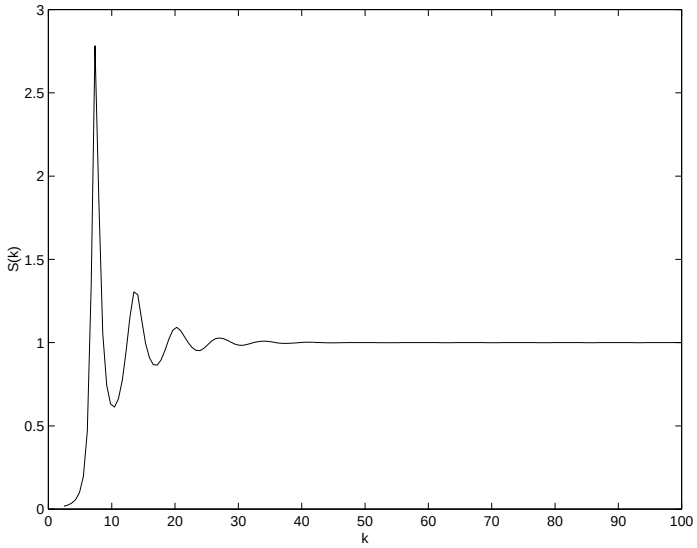

(b)

Figure 4. (a) Structure factor for the Yukawa fluid at $T^* = 1.3 \times 10^{-4}$ and $\lambda = 6.2$. (b) Structure factor for the $n = 6$ power law fluid at $X = 1.65$.

Hence, a greater structure factor leads to a greater $c(k)$ value and a lower weighted density in equation (7), providing a greater possibility that a solid phase can be stabilized. The structure factors generated by the PHNC integral equation for the $n = 6$ power law and the Yukawa $\lambda = 6.2$ ($T^* = 1.3 \times 10^{-4}$) fluids at their predicted crystallization densities into FCC solids are shown in figure 4. As can be seen, the first peak has a magnitude of slightly over 2.8 for the $n = 6$ power law fluid at $X = 1.65$. This is very close to the Hansen–Verlet rule value, especially considering the fact that computer simulations yield a range of crystallization

densities for this system from $X = 1.63$ to $X = 1.66$ [24, 25]. As a comparison, Kang and Ree report a first peak magnitude of 2.89 for the $n = 6$ fluid at crystallization [14]. For the Yukawa fluid, however, the value of the first peak of the structure factor we find is nearly 3.0 for $T^* = 1.3 \times 10^{-4}$ and a density of 0.0087, in excess of the value predicted by the Hansen-Verlet rule. Furthermore, our MWDA model underpredicts the coexisting densities; computer simulations indicate the true crystallization density is around 0.01 [15, 26]. Thus, at that density, the first peak of the structure factor would exceed three.

4. Other theories and experiments

In general, our results for the fluid–FCC and fluid–BCC transitions agree with computer simulations for both the power law [24, 25, 27–30] and Yukawa [15, 26, 31, 32] systems. In addition, our Yukawa phase diagram is qualitatively consistent with experimental studies on colloidal systems, and quantitatively close if the appropriate rescaling of charges is performed [33]. Errors in the fluid–solid coexisting densities compared with simulation studies follow the similar pattern of being greater as the potential becomes softer. For example, our errors in the power law system range from 3–4% for $n = 12$ to 8% and 12% for the $n = 4$ FCC and BCC transitions, respectively [9]. Similarly, the errors in λ for the Yukawa system range from 2% for $\lambda \sim 7$ to 10–17% for $\lambda \sim 4$. In all of the numbers above, the smaller errors are incurred when the Einstein vibrations are taken into account [11].

One recurring theme in our MWDA studies is the underprediction of coexisting densities compared with computer simulations for softer systems, especially in the Yukawa case, resulting in a greater area of solid stability in the phase diagram. While the computer simulation studies in the power law system were performed until crystallization occurred, the Yukawa fluid–solid transition line in the computer simulation study of Robbins, Kremer and Grest was determined by setting a constant Lindemann ratio of $L = 0.19$ [15, 26]. This assumption is not consistent with the power law simulation results, which predict varying Lindemann ratios of $L = 0.14$ for $n = 12$ to $L = 0.18$ for $n = 4$. A larger Lindemann constant would predict, *ceteris paribus*, lower coexisting densities and a greater range of solid stability.

This conclusion for the Yukawa system is supported by the Hansen–Verlet rule. While both the Lindemann and Hansen–Verlet rules should be taken as empirical and not absolute criteria for melting or freezing behaviour, the larger deviations of the Yukawa system again indicate that perhaps the region of solid stability is greater than that previously thought. Indeed, the large Hansen–Verlet first peak values we find are not unusual for the Yukawa system and in fact smaller than those found by some other investigators. Robbins *et al* find many Yukawa systems with structure factor first peak values of three or greater [15].

The miscibility gaps, or fractional changes in densities upon crystallization, that we find agree well with computer simulation studies for the power law case [24, 25, 27–30]. While the Yukawa density jumps generally agree with computer simulation studies [31, 32] and a more detailed study by Graf and Lowen [33], there is often substantial disagreement with experimental results. In a study of highly charged polystyrene latex crystallizing into a FCC solid, fractional density changes of around 0.76 are found [34-35]. These values are an order of magnitude greater than would be expected for the Yukawa system and could provide evidence of van der Waals instabilities in charged colloidal systems [36, 37]. An earlier work by Hachisu *et al* also finds a broad coexistence region, with the solid phase being 1.2 to 1.4 times as dense as the fluid phase [38]. This translates into a fractional change in density of around 0.17 to 0.29, still a factor of at least three too large for any simple Yukawa freezing model.

In summary, while there is no general rule for the position of the liquid–solid phase boundary, nor the liquid–BCC–FCC triple point, some interesting comparisons between

various soft sphere models can be made. The Lindemann parameter at the melting point and the height of the first peak of the crystallization liquid structure factor provide some insights into the nature of the structures near the freezing transition. The miscibility gap or density jump upon crystallization is another sensitive measure of phase behaviour and may indicate the inadequacy of some soft sphere potentials to model complex fluids.

Acknowledgment

This work was supported by National Science Foundation (NSF) grant No CTS-9413883.

References

[1] Van Megan W and Snook I 1984 *Adv. Colloid Interface Sci.* **21** 119
[2] Russell W B, Saville D A and Schowalter W R 1989 *Colloidal Suspensions* (Cambridge: Cambridge University Press)
[3] Kahl G 1980 *J. Chem. Phys.* **93** 5105
[4] Kahl G and Hafner J 1987 *Phys. Chem. Liquids* **17** 139
[5] Kahl G and Hafner J 1987 *Phys. Chem. Liquids* **17** 267
[6] Hansen J-P 1970 *Phys. Rev.* A **2** 221
[7] Young D A and Rogers F J 1984 *J. Chem. Phys.* **81** 2789
[8] Ross M 1979 *J. Chem. Phys.* **71** 1567
[9] Wang D C and Gast A P 1999 *J. Chem. Phys.* **110** 2522
[10] Wang D C and Gast A P 1999 *Phys. Rev.* E **59** 3964
[11] Wang D C and Gast A P *J. Chem. Phys.* at press
[12] Denton A R and Ashcroft N W 1989 *Phys. Rev.* A **39** 470
[13] Curtin W A and Ashcroft N W 1985 *Phys. Rev.* A **32** 2909
[14] Kang H S and Ree F H 1995 *J. Chem. Phys.* **103** 3629
[15] Robbins M O, Kremer K and Grest G S 1988 *J. Chem. Phys.* **88** 3286
[16] Hansen J-P 1973 *Phys. Rev.* A **8** 3096
[17] Pollack E L and Hansen J-P 1973 *Phys. Rev.* A **8** 3110
[18] Lindemann F A 1910 *Z. Phys.* **11** 609
[19] Alder B J and Wainwright T E 1959 *J. Chem. Phys.* **31** 459
[20] Young D A and Alder B J 1974 *J. Chem. Phys.* **60** 1254
[21] Hansen J-P and Verlet L 1969 *Phys. Rev.* **184** 151
[22] Verlet L 1968 *Phys. Rev.* **165** 201
[23] Hansen J-P and MacDonald I R 1986 *Theory of Simple Liquids* 2nd edn (New York: Academic)
[24] Agrawal R and Kofke D 1995 *Phys. Rev. Lett.* **74** 122
[25] Laird B B and Haymet A D J 1992 *Mol. Phys.* **75** 71
[26] Kremer K, Robbins M O and Grest G S 1986 *Phys. Rev. Lett.* **57** 2694
[27] Hoover W G, Ross M, Johnson K W, Henderson D, Barker J A and Brown B C 1970 *J. Chem. Phys.* **52** 4931
[28] Hoover W G and Ree F H 1968 *J. Chem. Phys.* **49** 3609
[29] Alder B J, Hoover W G and Young D A 1958 *J. Chem. Phys.* **49** 3688
[30] Ogura H, Matsuda H, Ogawa T, Ogita N and Veda A 1992 *Prog. Theor. Phys.* **58** 419
[31] Meijer E J and Frenkel D 1991 *J. Chem. Phys.* **94** 2269
[32] Rosenberg R O and Thirumalai D 1987 *Phys. Rev.* A **36** 5690
[33] Graf H and Lowen H 1998 *Phys. Rev.* E **57** 5744
[34] Monovoukas Y and Gast A P 1989 *J. Colloid Interface Sci.* **128** 533
[35] Gast A P and Monovoukas Y 1991 *Nature* **351** 553
[36] Netz R R and Orland H 1999 *Europhys. Lett.* **45** 726
[37] von Roij R, Dijkstra M and Hansen J-P 1999 *Phys. Rev.* E **59** 2010
[38] Hachisu S, Kobayashi Y and Kose A 1973 *J. Colloid Interface Sci.* **42** 342